Numerical Calculations of Wireless Power Transfer Coil Parameters

JONATAN NYSTRÖM
MASTER´S THESIS
DEPARTMENT OF ELECTRICAL AND INFORMATION TECHNOLOGY
FACULTY OF ENGINEERING | LTH | LUND UNIVERSITY

Numerical Calculations of Wireless Power Transfer Coil Parameters

Jonatan Nyström
`elt14jny@student.lu.se`

Department of Electrical and Information Technology
Lund University

Supervisor: Professor Buon Kiong Lau
`bkl@eit.lth.se`
Industrial Supervisor: Laurens Swaans
`ls@nok9.com`

Examiner: Professor Mats Gustafsson
`mats.gustafsson@eit.lth.se`

June 12, 2020

Abstract

Wireless Power Transfer (WPT) has become a commercially viable technology. The technology uses the phenomenon of electromagnetic induction between coils to transfer electrical power wirelessly. Due to the increasing interest in WPT, the need to understand how the power transfer between coils behaves in different settings, as well as the ability to simulate the process, have become increasingly important for further development of the technology.

This thesis investigates some of the existing methods for calculating the mutual inductance between coils. For arbitrarily wound coils the Neumann formula is used. And for taking the presence of ferrite plates into account an expression derived by Hurley and Duffy is used. The methods are implemented in Matlab [1] and compared to physical measurements and full-wave electromagnetic simulations made in the commercial software Ansys Maxwell [2].

The thesis focuses on 2 aspects: 1) The extent to which mutual inductance is affected by the presence of ferrites of varying size. The thesis shows that previously stated finite ferrite margins for expressions derived using the assumption of infinite ferrite plates in a magnetostatic setting, do not seem to hold for a simple two-coil system, and new margins are obtained. 2) The possibility of homogenizing the magnetic field for increased spatial coupling, using a multicoil array. The thesis shows that it is possible to increase the field homogeneity of an initial setup, at the cost of the field strength. It also finds that for a tri-coil system with coil centers forming an equilateral triangle, the optimal separation distance of the coil-centers in terms of providing a homogeneous field, is between 30% to 60% larger than the outer coil radius.

Acknowledgement

First and foremost I want to give my thanks to my beloved partner Emma for always being there for me, patiently listening to all my troubles and hardships. Without her, this thesis would not have happened. Secondly, I wish to express my deepest gratitude towards my industrial supervisor Laurens Swaans, CTO at nok9, and all the people there, for giving me the opportunity to write this thesis and for supplying much needed hardware, knowledge and advice. I would also like to sincerely thank and acknowledge my academic supervisor, Professor Buon Kiong Lau, for putting in so much time and hard work in reading and making well-thought suggestions on the thesis, as well as for his general encouragement and support.

Table of Contents

List of Figures

List of Tables

x

Introduction

1.1 Background

The application of Wireless Power Transfer (WPT) has been increasing rapidly the last couple of years, and the trend is expected to continue in the next few years, according to a report from IHS Markit (see Figure 1.1) [3].
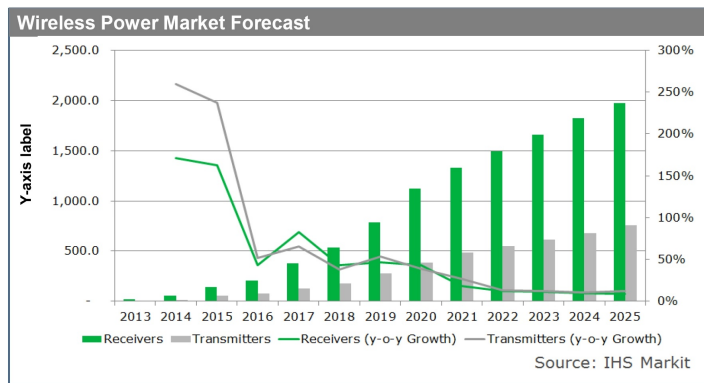
Figure 1.1: Historic and predicted market size of WPT. Source: [3]

Mobile phones and small electronic devices are already making use of this technology for battery charging. The current dominant WPT standard for small devices, the Qi Specification, has enabled devices from different manufacturers to interoperate, speeding up the spread of WPT technology.

In the future, WPT is also expected to play an increasingly important role for charging larger and more power-demanding devices such as laptops. A big advantage of WPT is the convenience and freedom of being able to easily charge your device, without being physically restrained by a wire. Wireless power charging also enables the possibility of removing the connector used for battery charging. This opens up the possibility of making the devices waterproof even during charging.

In principle, inductive WPT is based on the theory of electromagnetic induction, first discovered by Michael Faraday in the 19th century. It shares the same physics as a power transformer, which also relies on magnetic fields to transfer energy from the transmitter coil to the receiver coil.

The main difference between WPT and a transformer is that, in WPT, the transmitter and receiver share an "air core" where the magnetic field lines disperse quickly. In a traditional transformer, the core is made of a ferromagnetic material that "guides" the magnetic field lines, retaining a high field density as well as field uniformity (see Figures 1.2 and 1.3).
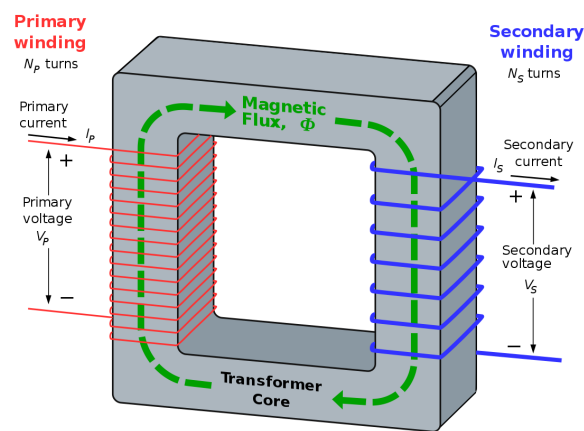
Figure 1.2: Magnetic field lines in a traditional ferrite-core transformer. Source: [4]
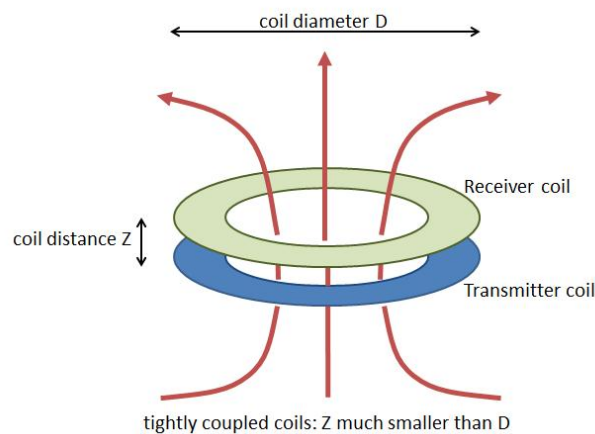
Figure 1.3: Magnetic field lines in a WPT setting with an air-core. Source: [5]

Hence, unlike a transformer, WPT coils should be perfectly aligned and placed close to each other, such that the distance z between them is small compared to the diameter of the coil (see Figure 1.3), in order for the magnetic flux generated by the transmitter to be "captured" by the receiver, i.e., to be tightly coupled. Nevertheless, the ability to avoid physical wire connections still provides convenience to users, and WPT also enables other new features as previously discussed.

According to the theory of electromagnetic induction, the relationship between the current in the transmitter coil and the induced voltage in the receiver coil is governed by the mutual inductance between the coils. In particular the induced voltage is given by

$$V_{emf} = -\frac{d\Phi}{dt},\qquad(1.1)$$

where the magnetic flux Φ is the product of the current i(t) and the mutual inductance M, i.e., $\Phi = i(t) \cdot M$.

Due to the spatial freedom enabled by WPT, it is of interest to create transmitter coils with good enough coupling when the receiver coil is not perfectly aligned. One way of addressing this is to introduce a multi-coil transmitter system. For example, if all the coils are simultaneously energized, then each of the coils, if spatially displaced from one another, will provide a strong magnetic field over a larger spatial region, which will allow more freedom in the movement of the receiver and its coil without experiencing a significant change in the coupling level.

There are several expressions derived for calculating the mutual inductance in air, between loops of filamentary or circular/rectangular cross-section, since the late 19th century [6],[7],[8]. However, newer expressions have been derived to take into account the presence of different materials with magnetic properties [9], [10], in our case ferrite. This is much closer to the practical situation of WPT, where two ferrite plates "sandwich" the transmitter and receiver coils to enhance/amplify the transmitted power/magnetic field. The amplification arises due to boundary conditions imposed by the air-ferrite interface [11].

1.2   Goals of the Thesis

The overarching goal, for researching the subject, is to be able to calculate the self-/mutual inductance of the WPT coil-system within minutes for any arbitrarily positioned transmitter and receiver coils in space. The research should take into account the presence of magnetic materials, also arbitrarily positioned.

However, the goal of this thesis is to identify dominant parameters governing the resulting mutual inductance for some specific WPT coil configurations. In addition, the thesis tries to quantify the errors caused by various approximations and assumptions.

Furthermore the thesis examines the possibility of increasing the spatial reach for good coupling by attempting to equalize the magnetic field in the xy-plane (i.e., a horizontal area) using a multi-coil setup. Once a solution to this is found for a certain symmetric configuration of coils (a unit cell), this solution can be easily expanded by simply adding coils next to each other in the same pattern, like a honeycomb. This will give a large area of good coupling. Hence the idea is that the charger detects a device at a certain position and then simply activates the corresponding coils for WPT.

1.3   Structure of the Thesis

The thesis focuses on determining the mutual inductance of WPT coils in different settings using numerical computations in Matlab, physical measurements and full-wave simulations in Ansys Maxwell. In Chapter 1, the background of WPT is given and the motivation and goal of the thesis are described. In Chapter 2, the theory used in the thesis is presented. The WPT coil systems used in this study and the corresponding simulation/measurement setups for these coil systems are defined in Chapter 3. In Chapter 4, the numerical and full-wave simulation results, as well as measurement results, are presented and discussed. In Chapter 5, a summary of the thesis and its main results are presented. Possible future work is discussed.

Theory

In this chapter theoretical concepts used in the thesis are defined and explained.

2.1 Material Properties

Throughout this paper, all materials are assumed to be linear and homogeneous with regard to conductivity and permeability, such that these material properties can be taken as constants. Conductors are assumed to be perfect conductors, i.e., $\sigma = \infty$. Skin-effects and proximity effects for the wires are not addressed in the thesis. An example of a study addressing these practical aspects is [12].

Moreover, the phenomenon of hysteresis and magnetic saturation is not addressed in the calculations performed for this thesis. An example of a study addressing this issue is [13], which models the hysteresis losses using complex permeability in a WPT-setting.

Magnetic permeability μ [H/m], is a magnetic material property that can be interpreted as how magnetized the material becomes due to an external magnetic field. The permeability of vacuum is: $\mu_0 = 4\pi \times 10^{-7}$ [H/m].The permeability of any material μ, is often expressed as the permeability of vacuum times a factor called relative permeability μ_r, giving $\mu = \mu_0 \mu_r$. The permeability for vacuum and air is almost the same and throughout this thesis it will be assumed, for simplicity, that they are the same.

Electric conductivity σ [S/m], of a material, can be understood as a measure on how well the material conducts electric current. It is the inverse of electric resistivity, ρ [Ωm].

2.2   Coil Parameters

2.2.1   Coil Inductance

Mutual inductance M[H], between two closed conducting one-turn coils is the relation between the magnetic flux $\Phi_{1,2}$ going through the loop area S_2 of a receiver coil 2, and the steady current I_1, running through the transmitter coil 1, with the latter generating a magnetic field B_1, $M = \Phi_{1,2}/I_1$ [11], where

$$\Phi_{1,2} = \int_{S_2} \vec{B_1} \cdot \vec{ds_2},$$

or alternatively expressed (by Stoke's theorem) via magnetic vector potential $\vec{A}$ [11]

$$\Phi_{1,2} = \oint_{C_2} \vec{A_1} \cdot \vec{dl_2}, \tag{2.1}$$

where C_2 denotes the boundary of the surface S_2. For the case of alternating current in the transmitter coil, mutual inductance results in electromotive force (EMF) being induced in the receiver coil due to Faraday's Law of Electromagnetic Induction.

Self-inductance L[H] can in the same way, be viewed as the relationship between the magnetic flux through the same coil as the coil with the current that generates the magnetic flux. In other words, self-inductance is the total amount of magnetic flux generated by the coil per unit current.

For the alternating current case, the inductance will be a measure on how "hard" it is to drive a current through the coil, i.e., it is directly proportional to the reactance, the complex part of the impedance Z.

2.2.2   Inductance of Multi-turn Loops

Although most expressions for inductance are derived for one-turn loops, in reality, coils are not just one-turn loops. Most often they are spirals and or solenoids, i.e., a continuous "trace" of a wound wire.

One way of handling this is to let one loop (chosen appropriately) represent the entire coil and then just multiply the result (e.g., flux passing through the loop) by the number of turns of the coil, i.e., the idea of flux linkage $\Lambda_{1,1} = N_1\Phi_{1,1}$, [11]. This approach assumes that the representative loop has an "average" behavior. This simple approach makes a lot of sense for calculating the self-inductance of a solenoidal coil in air, since if it is not too long, almost all flux lines generated by each loop also pass through all the other loops.

However, for a flat spiral coil, the inner turns will generate flux lines that cancel some of the flux generated by the outer ones. And when finite ferrite plates are introduced, the flux lines from the inner coils will be more amplified than the outer ones (since the inner ones are further away from the edges of the ferrite plates). This raises questions on how well this approximation works and how one would go about choosing "representative" loops.

Instead, to find the inductance, one can use the principle of superposition. The multi-turn coil is approximated as a system of one-turn loops. Then, the inductance is calculated as follows [14]

$$L = \sum_{i=j}^{N_2} \sum_{i=1}^{N_1} L_{i,j},$$ (2.2)

where $L_{i,i}$ is the self-inductance of one-turn loop i and $L_{i,j}$ is the mutual inductance between loops i and j. Note that this expression can be used both for the self-inductance of a multi-turn coil (where the mutual inductance is added twice for each corresponding pair of loops) and the mutual inductance between two different multi-turn coils.

2.2.3 Coil Impedance

Impedance $Z = U/I = R + jX$, is the relationship between the voltage and the current signals. When the impedance is taken across the coil terminals, R is the equivalent coil resistance. For an ideal coil with self-inductance L, the reactance $X = \omega L$. Note that this term changes with the frequency ω of the signals. The equivalent circuit for a coil is depicted in Figure 2.1.
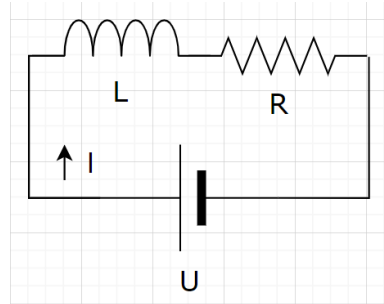
Figure 2.1: Equivalent circuit elements for a coil, with a voltage source U attached across the coil terminals and current I flowing in the coil.

2.2.4 Coupling Factor

The coupling factor is a measure of how efficiently the magnetic flux generated in one coil is received in the other. It is indicative of how well the system can transfer power. The coupling factor can be expressed in terms of the mutual inductance M between the two coils and their respective self-inductance L_1 and L_2

$$k = \frac{M}{\sqrt{L_1 \cdot L_2}}.$$ (2.3)

The metric can also be interpreted as how strongly the two coils are "paired" electromagnetically.

2.3 Calculation of Mutual Inductance

2.3.1 Mutual Inductance in Air

Since air and vacuum have almost the same permeability, the permeability for vacuum, μ_0, will be used for air subsequently in this thesis. The mutual inductance between two concentric filamentary loops of radius a and r respectively, at a distance of z from each other (see Figure 2.2) can be expressed as [9]

$$M = \mu_0 \pi ar \int_{k=0}^{\infty} J_1(kr) J_1(ka) e^{-kz} \cdot dk, \tag{2.4}$$

where J_i is an i:th order bessel function of the first kind. Note that this quantity is independent of the frequency and magnitude of the current running through the filament. This integral (2.4) can be evaluated using elliptic integrals as [9]

$$M = \mu_0 \sqrt{4ar} \frac{1}{K(a,r,z)} \Psi(K(a,r,z)), \tag{2.5}$$

where: $K^2(a,r,z) = \frac{4ar}{z^2+(a+r)^2}, \Psi(k) = (1 - \frac{k^2}{2}) K_e(k) - E_e(k)$,
K_e and E_e are complete elliptic integrals of first- and second kind.
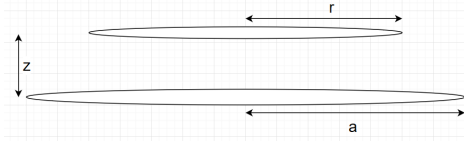
Figure 2.2: Basic two filamentary loops system

2.3.2 The Neumann Formula

The Neumann formula gives the mutual inductance between two arbitrary filamentary DC-current paths [11]. It uses Biot-Savart's law to find the magnetic vector potential at a point due to a current of magnitude I in a differential line-segment $\vec{dl}$ (also implying the direction of the current), adding each segment's contribution according to the superposition principle. The result is then combined with (2.1) to yield the formula. The expression turns out to only depend on the distances between the differential line-segments along the traces ($R_{1,2}$) and the line segments direction, i.e.,

$$M = \frac{\mu_0}{4\pi} \oint_{C_2} \oint_{C_1} \frac{1}{R_{1,2}} \vec{dl}_1 \cdot \vec{dl}_2. \tag{2.6}$$

The double integral can be numerically approximated by

$$M \approx \frac{\mu_0}{4\pi} \sum_{j=1}^{N_2} \sum_{i=1}^{N_1} \frac{1}{R_{i,j}} \vec{dl}_i \cdot \vec{dl}_j, \tag{2.7}$$

where N_2, N_1 are the number of points (the vector between two points define a line segment) used to describe the trace of coil 2 and coil 1, respectively. $R_{i,j}$ is the

distance between the points i and j. $\vec{dl}_i$ is the differential line-segment pointing from point i to point $i+1$, i.e., the next point along the trace ($\vec{dl}_j$ is similarly defined).

The number of calculations required depends on the number of points used to describe the two traces ($N_{calc} \sim N_2 \cdot N_1$) and its choice involves a trade-off between accuracy and computational cost.

2.3.3 Mutual Inductance with Ferrite Plates

In almost all Qi WPT-systems, the transmitter and receiver coils each have a ferrite plate "behind" it, creating a "sandwich" structure when the two coils are brought close to each other. This amplifies the magnetic field on the coil side due to the boundary conditions imposed by the ferrites, and hence the mutual inductance also increases. The ferrite plates also shields electronics on the other side of each plate and focuses the magnetic field, reducing magnetic field leakage. Due to the effect of the ferrite plates on the magnetic field, there is a need to include them in the calculation for the mutual inductance.

Ferrite Plates and Mutual Impedance

In [9] and [15], William Gerard Hurley and Maeve C. Duffy develop an expression of the mutual impedance $Z_{1,2}$, between two concentric, one-turn loops of rectangular cross-section with ferrite plates extending to infinity, but with finite thickness, above and below the loops, as shown in Figure 2.3.
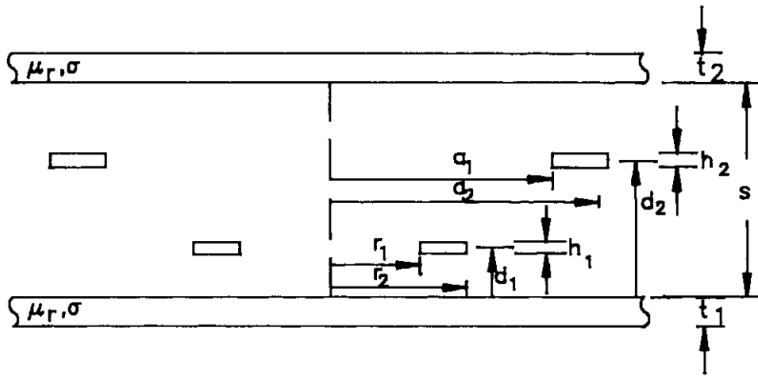

Figure 2.3: Hurley-Duffys basic one-turn coil setup. Source: [9]

The basic idea of the method is to divide the mutual impedance between the coils into two parts. The impedance without the ferrite $j\omega M_{air}$ and the impedance due to the presence of the ferrite Z_{sw}^p, as seen in (2.8)

$$Z_{1,2} = jwM_{air} + Z_{sw}^p = R + jwL_{1,2}^{total} \tag{2.8}$$

where M_{air} is the mutual inductance between the coils without ferrites.
The definition of Z_{sw}^p, is provided in Appendix A. This gives the total mutual inductance

$$M_{tot} = L_{1,2}^{total} = \frac{Im(Z_{1,2})}{\omega} \tag{2.9}$$

The mutual inductance without the ferrites M_{air} can be calculated for wires of rectangular cross-section as well. However, the numerical integral for this expression converges slowly [9] and hence Hurley and Duffy choose to approximate this quantity with the filament-based expression in (2.5). Ideally, the filament is placed at the "center point" of the actual, distributed current flow, i.e., such that the filament is surrounded by the same current density over the wire cross-section (approximately true for Litz wire used in WPT coils). The implementation for this thesis will stick to this convention and will place the filament at the geometric mean of the inner and outer radii of a finite cross-section wire to the coil center. Since this approach has been shown to provide a good approximation [9].

2.4   Physical Measurements

In this work, the physical measurements of the mutual inductance were made by connecting the coils in series in different configurations, such that the self-inductance of the system of each configuration was measured. First the orientation/polarization of the coils were arranged to oppose each other (i.e., the magnetic fields generated by the currents in the two coils were oppositely directed) and then the coils were connected such that the magnetic fields aided each other. The self-inductance of these two cases are measured as L_{aid} and L_{oppose}, respectively. The mutual inductance is then given by [16]

$$M = \frac{L_{aid} - L_{oppose}}{4}. \tag{2.10}$$

Setups and Implementation

In this chapter, the various coil system setups examined in the thesis are specified. The abbreviation "CC" is used to denote "center-to-center (distance)". Likewise "T2B" abbreviates "top-to-bottom (distance)". For the setups where frequency was taken into account, the frequency was chosen to be 100kHz unless otherwise stated. This is because the Qi Specification is operating at around that frequency.

Ansys Maxwell is an electromagnetic simulation software that is used in this thesis for various full-wave coil simulations. Ansys Maxwell uses the Finite Element Method (FEM) to solve fundamental electromagnetic equations from physics in a meshed space. Apart from electromagnetic simulations, analytical expressions used for calculating coil parameters (e.g., Neumann Formula) were implemented in Matlab. In addition, the data generated in Ansys Maxwell was exported to Matlab for plotting.

All electromagnetic simulations in Ansys Maxwell were done for solid wire, i.e., non-uniform current distribution, of circular cross-section, unless otherwise stated. Also, unless otherwise stated, all coils with circular cross-section were assumed to have a wire diameter, "dWire", of 1mm. For the wires with a square cross-section, the side-length x was chosen to be 0.886mm (giving the same cross-section area). The distance between the closest neighbouring wires (in empty space) was set to 0.1mm.

For setups 1 and 2, the inner diameter was measured over the inner empty area i.e., not including any wire-thickness. The outer diameter was measured over entire coil area i.e., including thickness of outer wire. Five different setups were used, which involved some combinations of electromagnetic simulations in Ansys Maxwell, analytical computations using Matlab, as well as physical measurements. The purposes and the methods used for the five setups are summarized in Table 3.1.

Setup	Description
1	Aims to equalize the mutual inductance between a multi-coil transmitter (Tx) and a small receiver (Rx) coil over a region between the coils, by adjusting the number of turns in the Tx coils. A Matlab script implementing the Neumann formula was used to calculate the mutual inductance. No ferrite was used.
2	Aims to find a linear relationship between the mutual inductance for misaligned Tx-Rx coil pairs and the shared coil area. The setup considered ferrite plates "behind" the coils and the mutual inductance was obtained using magnetostatic simulations on Ansys Maxwell.
3	Aims to study the impact of the ferrite size on mutual inductance, for a simplified ferrite-backed coil pair with one turn each. As in setup 2, the mutual inductance was obtained from simulation using Ansys Maxwell.
4	Aims to validate the Matlab implementation of the mutual inductance expression in Hurley and Duffy's paper [9], which accounts for the presence of ferrite plates. Both Matlab and Ansys Maxwell simulations were used.
5	Aims to find the minimum ferrite plate size that well approximates the infinite ferrite assumptions, when it comes to obtaining the mutual inductance for a realistic coil configuration. Both Ansys Maxwell simulation and physical measurement were used for this part.

Table 3.1: Descriptions of the five setups considered

3.1   Setup 1: Multi-coil

In this setup the magnitude of the magnetic field (B field) in the z-direction was mapped for a three-coil transmitter coil system, over a grid of positions, using the mutual inductance, M, of a small receiver coil as a proxy. Even though the actual quantity obtained is the mutual inductance, this quantity is a scaled version of the magnetic field in a region (assuming transmitter coil current of 1 A), which approximates the field at a point when the receiver coil is very small.

Then, a measure of the homogeneity of M for a smaller inner grid, was calculated and compared for different spacings between the coils and different combinations of number of turns on the coils. The values were simulated in Matlab using the approximated Neumann formula, given by (2.7).

Coil Configuration

Three-coil Transmitter (Tx):
The simulated model of the three-coil system is based on a physical counterpart, depicted in Figures. 3.1 and 3.2. The three spiral coils are partially stacked on top of each other, with each coil having two layers. If all coil axes are aligned along the z axis (though at different xy planes), then the centers of the three coils form the corners of an equilateral triangle (with the side length of 25 mm).

It is noted that the wire used to form each coil is represented by a line tracing the length of the coil, which allows for the Neumann formula to be used for calculating mutual inductance. The vertical spacing between these neighboring line paths is 1.1mm. Of which 1mm corresponds to the assumed thickness of the wire, and 0.1mm is the spacing (in air) between the outer edges of the wires, in two adjacent layers. The outer diameter of each spiral coil is 39mm. The numbers of turns and inner diameters of the Tx coils are given in Table 3.2.

	Turns	Inner diameter
Tx low 3	7	22mm
Tx mid 2	8	19mm
Tx high 1	9	18mm

Table 3.2: Tx coil parameters

Receiver (Rx) coil:
The receiver coil is a one-loop circular coil, chosen to have an area of 1cm^2, giving a radius of approximately 5.64mm. The size of the chosen receiver coil, represents a trade-off between having good spatial resolution and quick calculations (i.e., a small area) vs. a good numerical approximation (i.e., having a large circumference in relation to the resolution of 0.1mm between each point, used in the integral calculation).

Tx-Rx coil system:
The multi-coil case of setup 1 was implemented in Matlab, where the Tx coil system and the Rx coil loop were both constructed as continuous traces in xyz-coordinates with equidistant points. The spatial resolution, i.e., the distance between each point, i.e., the length of each line segment $|\vec{dl}|$ described in Section 2.3.2, was chosen to be 0.1mm. This line segment length is equivalent of roughly 0.04% of the outer circumference of one Tx coil and roughly 0.14% of that of the the Rx coil. A "terminal" for the Tx coil trace was added with the length of one outer radius (19.5mm). The other terminal as well as connecting wires between the three coils are also added (see Figure 3.1 for details). The final Tx coil trace of the entire system consists of 44808 points in space and the Rx coil trace consists of 355 points.

The mutual inductance was calculated for a range of center positions of the Rx coil. The center positions consist of a square grid of 15x15 equidistant points, centered at the origin. From -19.5mm to 19.5mm for the x and y dimensions, respectively, i.e., with 39mm corresponding to the outer diameter of any one coil in the Tx spiral coil system. This gives a grid spacing of 2.8mm, which is roughly 25% of the Rx coil diameter. Note that this means that the Rx coil is receiving some of the same flux lines at neighbouring positions.

The Rx coil was placed below the Tx coil system, i.e., such that the Tx coil furthest away (top most Tx coil) was given the most turns (compensating for its larger distance to the Rx coil), as can be seen in Table 3.2. The separation distance between the lower surface of the Tx coil system and the upper surface is 3 mm (i.e., T2B distance).
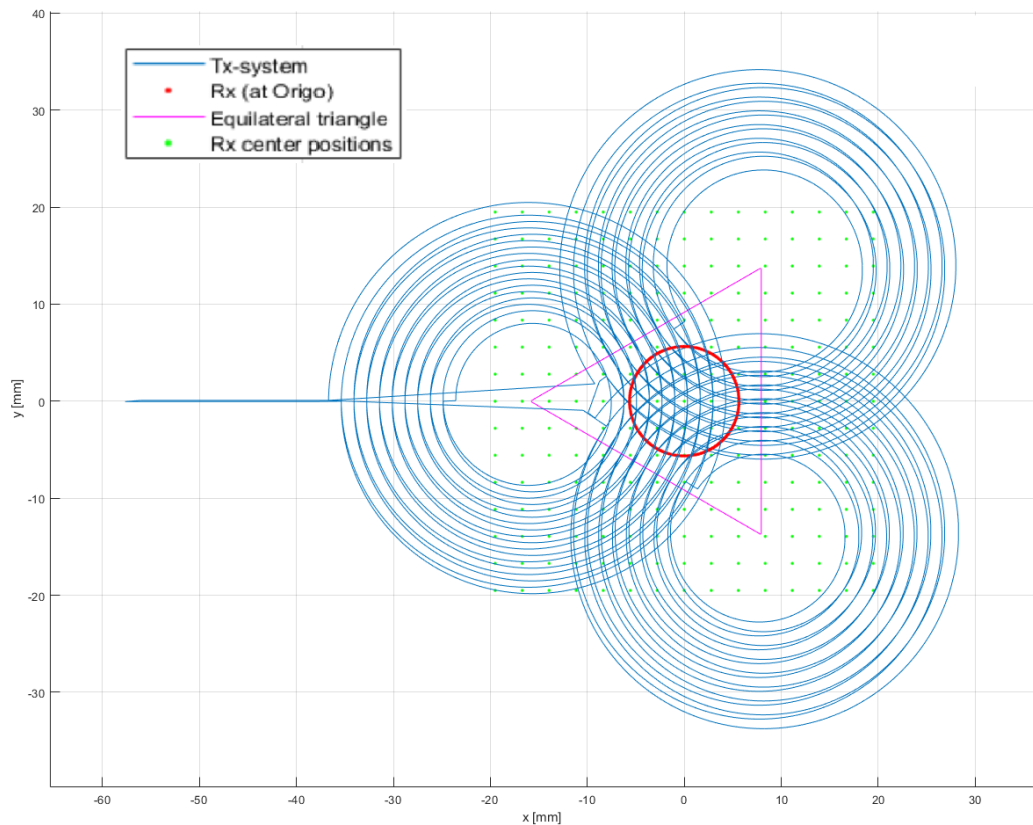
Figure 3.1: System of large Tx coils and a small Rx loop as viewed from above
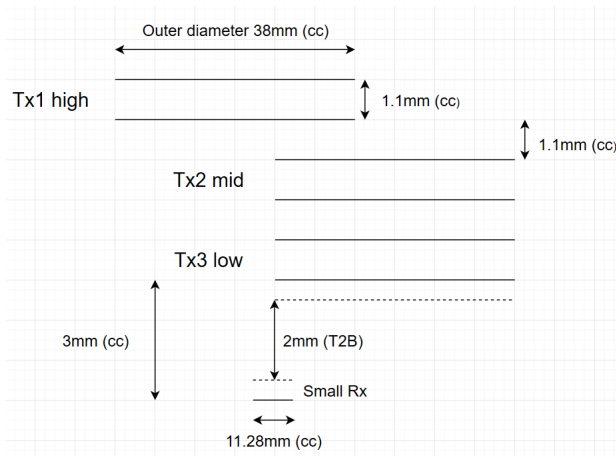
Figure 3.2: Conceptual image of the Tx and Rx coils as seen from the side (showing only the line trace along the center of the wires of the coils)

The dashed lines in Figure 3.2 represent the edge of the wire and the solid lines the center of the wires.

3.1.1 Equalize B field

The goal of the setup was to test if it was possible to equalize the B field by adding or reducing the number of inner turns on the coils (keeping the outer diameter constant). Several variations of the number of turns in the initial setup were tested, which also changed the number of points used in the trace.

The corresponding mutual inductance map was plotted. The mean and standard deviation of the 49 inner position points, and their ratio were calculated, with the ratio being taken as a measure on the homogeneity of the data. These 49 points correspond to the center point at the origin $\pm$ 3 points in the x and y directions (hence 7×7 grid points). The outer-most point is 8.36mm + receiver radius 5.64mm = 14mm. Hence these 49 points roughly span an inner square area of 28×28mm centered at the origin.

The reason for using the ratio between mean and standard deviation as a measure of the homogeneity is to make field homogeneity comparable for different means and setups. The standard deviation is a typical measure of how much the data points deviates from the mean value. The choice of the 49 grid points was somewhat arbitrary and this aspect could be improved for further work. From a modular perspective it is important that the area being equalized, covers much of the transmitter coils' overlapping surface such that there is no "hole" with unexpected mutual inductance behavior between the two neighbouring Tx modules (each having the Tx multi-coil system).

The entire setup 1 was also tested for a slightly larger side length of 27.5mm, for the equilateral triangle formed by the coil centers. This corresponds to moving the three Tx coils a bit further away from each other in the xy-plane.

3.2   Setup 2: Shared Area

The aim of the setup was to find a linear relationship between the shared area of two coils and their mutual inductance. This was motivated partly by the fact that the magnetic field (generated by the transmitter coil) weakens quickly outside of the two field-enhancing ferrite plates. If the field within the inner area of the transmitter coil is fairly homogeneous, the mutual inductance should just be the mutual inductance for the perfectly aligned case, scaled by a factor of the percentage shared area. This idea of a scaling factor based on the shared area will henceforth be referred to as the "shared area model" or "shared area principle". For larger distances in the z-direction between the transmitter and receiver coils, the magnetic field lines will both divert from one another and the field will weaken. Hence, this study was limited to small distances between the two coils in the z-direction.

Magnetostatic simulations was made using Ansys Maxwell for different receiver coil positions. The wire type was chosen to be stranded (giving a uniform current distribution in the wires). For the transmitter coil, three separate loops were used to approximate a three-turn spiral configuration, with the loops having the radii of 20, 18.9 and 17.8mm (CC) respectively. The receiver was chosen as a one loop coil of radius 20mm (CC). The square ferrite plates on both transmitter and receiver coils had a thickness of 0.4mm and a side length of 2(radius+5mm) = 50mm, centered around the center of their respective coil (see Figure 3.3).
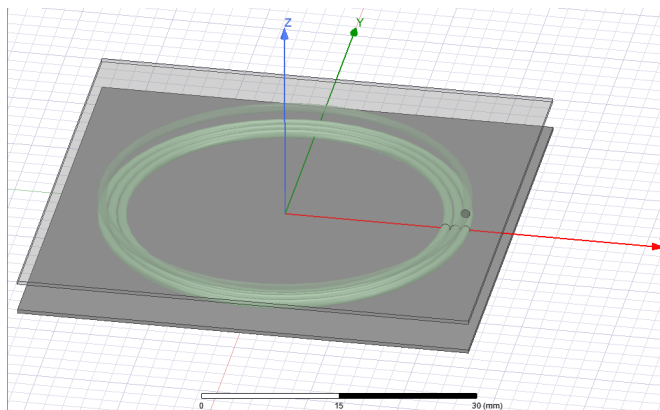

Figure 3.3: Simulation model of setup 2 in Ansys Maxwell

The center positions of the receiver coil were chosen as 0:2:30mm in the x-direction. The y position was fixed to 0 and the z position, as measured between the closest wires of the two coils, was set to 2mm (T2B). Here, 2mm corresponds to 1% of the Tx coil outer radius and 30mm to 150%.

The results from the Ansys Maxwell simulations were exported to Matlab and compared to the results calculated using the shared area principle. The Matlab implementation was based on the result of the case of concentric transmitter-receiver coil alignment from Ansys Maxwell.

3.3   Setup 3: Finite Ferrite

The aim of the setup was to study the impact of the presence of the ferrite plates. Magnetostatic simulations on the mutual inductance was made using Ansys Maxwell for different ferrite plate sizes. The wire type was set to stranded. The coil configuration consisted of two concentric loops of the same radii (10mm (CC)). Each with a corresponding ferrite plate of varying size "behind" them at a distance of 0.1mm (T2B). The separation between the loops was set to 2mm (CC) (10% of the coil diameter).

The width of the square ferrite plates was set to range from a factor 1 to 4 of the coil diameter, with a step size of 25% of the diameter, giving ferrite widths of 20:5:80mm. The thickness was set to range from a factor 0.5 to 3 of the wire diameter, with a step size of 50% (since the mutual inductance is less sensitive to this variable [9]). This corresponds to thicknesses of 0.5:0.5:3mm. Figure 3.4 shows the two cases of the smallest, thinnest versus the largest, thickest ferrite plates in relation to the coils.
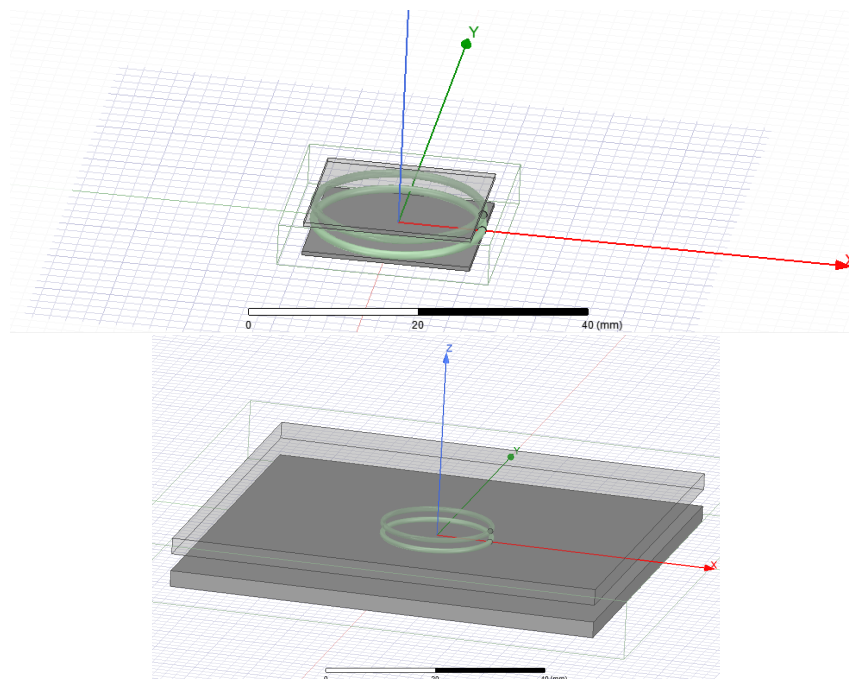
Figure 3.4: Smallest/thinnest vs. largest/thickest ferrite plates

3.4   Setup 4: Hurley-Duffy

The goal of the setup was to validate the implementation of the expression given by Hurley-Duffy in [9]. It is important to note that in this setup there is only one "sandwiched" coil for which the self-inductance is being calculated. The setup was simulated using Ansys Maxwell and calculated in Matlab using the implementation from the article. Both results were then compared with the results in the article.

Eddy current simulations were made in Ansys Maxwell for the frequencies of 100kHz and 100MHz, respectively. The wire type was set to solid. Both ferrite plates was chosen to have the same dimensions. Unfortunately the width of the ferrite plates is not clearly defined in the paper but it was assumed to be large in relation to the coil diameter. In this thesis, the ferrite was chosen to be 50% wider, which corresponds to 10.35mm. The ferrite thickness was set to 0.5mm. Conductivity σ and relative permeability μ_r of the ferrite used in the paper was 10[S/m] and 1000 respectively. In Figure 3.5, the detailed dimensions of the setup are defined. Note the rectangular cross section of the wires. Figure 3.6 shows the setup in Ansys Maxwell.
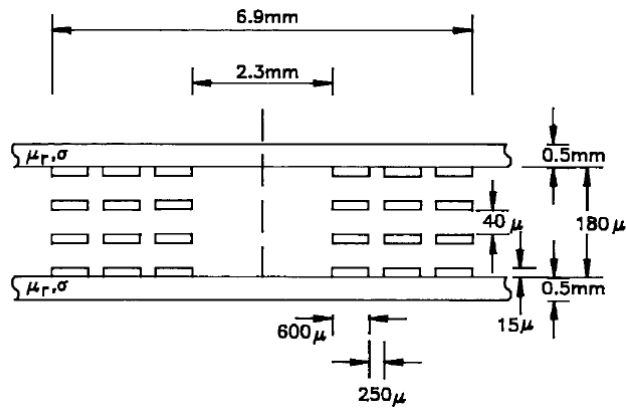
**Figure 3.5:** Sketch over the setup from the paper [9]
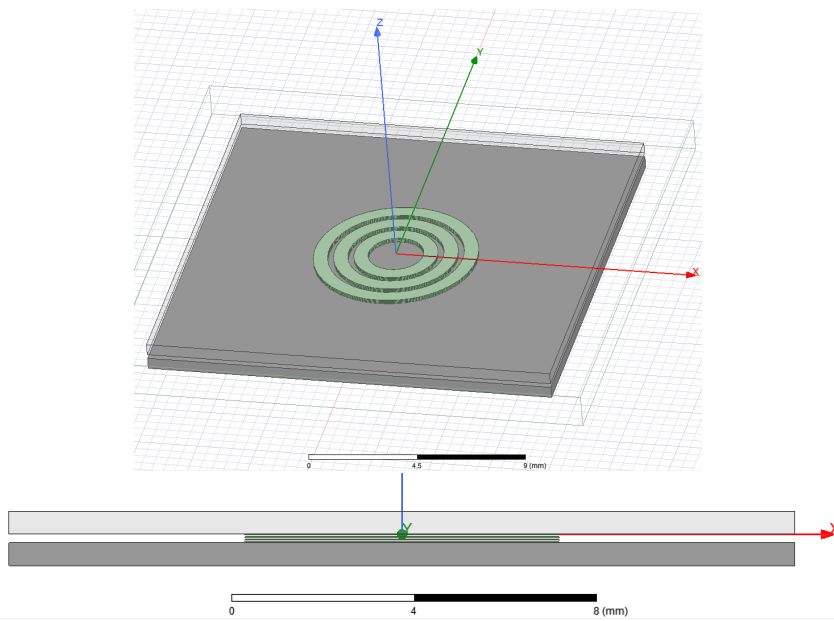
Figure 3.6: The coil setup in Ansys Maxwell

3.5   Setup 5: Physical 12-turn Spiral

Setup 5 had two identical coils "sandwiched" by a ferrite plate attached to each coil. Measurements on a physical setup as well as eddy current simulations in Ansys Maxwell on the setup were made and compared with each other. The physical setup was measured using the LCR-meter LCR-8101G. A feed signal of 500mVac at the frequency of 100kHz was used. The physical ferrite had an approximate conductivity σ and relative permeability μ_r of 0.01 [Siemens/m] and 1000 respectively. It is important to note that the physical electromagnetic properties of the ferrite changes with temperature, however in this thesis they are assumed to be constant. The ferrite plates had the dimensions of $51.7 \times 51.7 \times 2.5 \text{mm}^3$, i.e., the width was roughly 12% larger than the outer diameter of the coils. Table 3.3 gives the parameters of the coils used. The inner diameter was measured over the open inner area from edge-to-edge of the inner most wire, where as the outer diameter is measured from outer edges of the outer-most wire.

Type	Turns	Inner diameter	Outer diameter	wire diameter	Layers
Spiral	12	20mm	46mm	1mm	1

Table 3.3: Parameters of coil

In Figure 3.7, one can observe that the actual setup was not actually perfectly circular and that there was also a ferrite core in the middle to enhance the coupling, which was not included in the simulations.
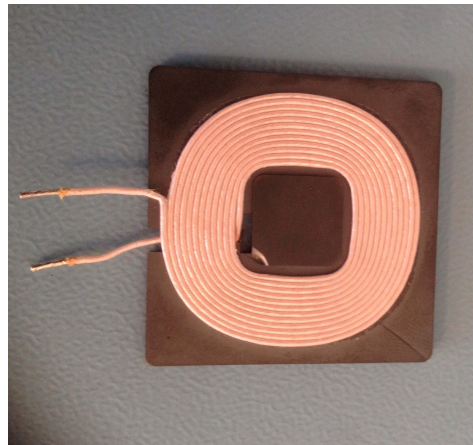

Figure 3.7: Physical coil

Figure 3.8 shows the setup in Ansys Maxwell.
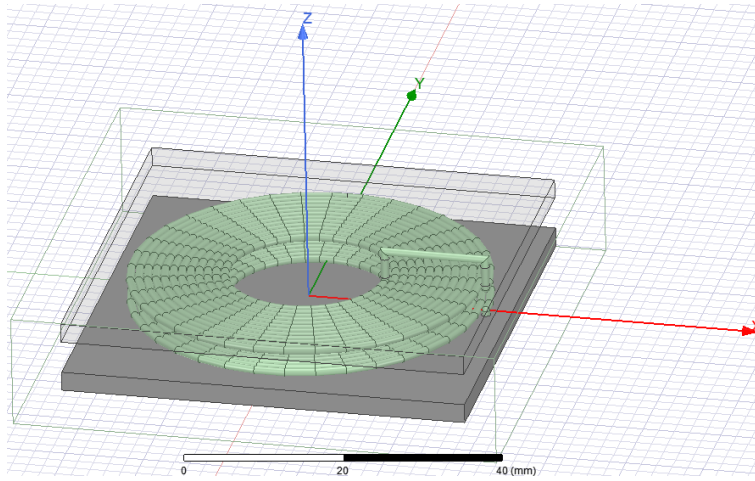
Figure 3.8: Setup in Ansys Maxwell

3.5.1   Misalignment

The expressions for the mutual inductance, taking the ferrites into account [9], assume infinite ferrite plates. So, strictly speaking, they cannot be used for misaligned coils with finite ferrite plates. This is due to both the infinite ferrite plate assumption not being satisfied as well as the asymmetry in the magnetic fields that arise due to the misalignment. The shared area principle was introduced as an attempt to capture how the mutual inductance is affected by misalignments for coils with finite ferrites. The goal was to test how well the shared area principle captures the behaviour of the mutual inductance for a more complicated practical setting (of misaligned coils) compared to the one in setup 2.

The receiver coil with its corresponding ferrite plate was misaligned in the x-direction by the spacings of 0:2:14mm. These values were chosen due to the limitations of the physical setup in range and resolution. The receiver coil was placed 2mm T2B (z-direction) from the transmitter, as measured between the closest wires of the coils. The results from simulations in Ansys Maxwell and the measured values were exported to Matlab where the shared area principle was used to calculate the mutual inductance. Several variations of scaling the concentric coils' mutual inductance value for misalignments were tested, using different combinations of the inner, outer and geometric mean radii of the coils to calculate the shared areas.

3.5.2   Ferrite Size

For the concentric coils case, i.e., no misalignment, the mutual inductance was calculated using equations (A.1) and (2.8) which assume infinite ferrite plates. The effect of the ferrite plate was examined by simulating the mutual inductance in Ansys Maxwell for varying ferrite sizes. The ferrite plate widths were chosen roughly as a factor 1 to 3 of the outer coil diameter, corresponding to ferrite plate widths of 52:7:143mm. The thickness was kept constant at 2.5mm. The goal was to see for what ferrite size the infinite assumption starts to become a reasonable approximation for a more complex practical coil configuration.

Results and Discussions

In this chapter the results of chapter 3 is presented and discussed.

4.1 Setup 1: Multi-coil

4.1.1 Computation time

The average computation time for the mutual inductance between the two traces, described in Chapter 3, using the Neumann formula was 0.2 seconds for 1 position of the receiver coil. This meant that the calculation of flux (mutual inductance) over the chosen area of interest ($1600mm^2$) or 225 positions of the receiver coil, took roughly 45 seconds. The actual computation times for each position can be viewed in Figure 4.1.
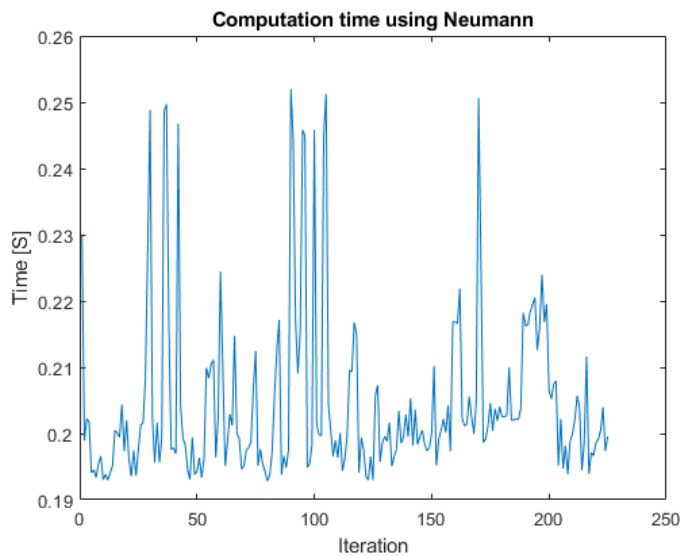

Figure 4.1: Computational times of Neumann formula for different Rx coil positions

The computational complexity should be the same regardless of where the receiver coil is positioned and hence one would expect a constant computational time. Most likely the spikes seen in Figure 4.1 is due to other programs or processes running at the same time on the computer.

4.1.2 Equalize B

Hypotenuse (distance between two coil centers): 25mm

Figure 4.2 shows a map of the mutual inductance for a small receiver and the initial transmitter coil system. The color and size of circles represent the magnitude of the mutual inductance measured at the position. The red square shows the boundary of the inner grid of points used to calculate the field homogeneity.
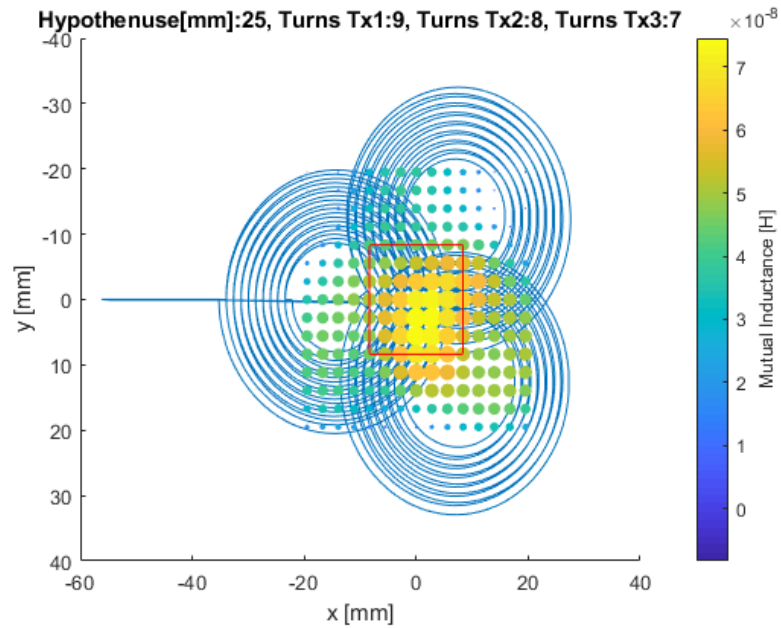
Figure 4.2: Map of mutual inductance for small receiver coil from setup 1. Initial setup with 9,8,7, Tx coil turns. Hypotenuse: 25mm

Just adding one or two inner turns as coils are positioned further from the receiver coil, does not seem to fully compensate for the reduced field strength due to the increased distance. Hence, we see that the field strength is skewed towards the closest (in z) Tx-coil (lower right). Tables 4.1 and 4.2 show the average and standard deviation of the mutual inductance, as well as their ratio, over all grid points and the inner grid points respectively.

Number of turns			Average Inductance	Standard deviation	ratio
Tx1 high	Tx2 mid	Tx3 low	μ_M (μH)	σ (μH)	σ/μ_M %
9	8	7	3.877	1.803	46.5
10	8	6	3.789	1.680	44.3
11	8	5	3.673	1.639	44.6
11	8	6	3.843	1.699	44.2
12	8	5	3.717	1.668	44.9
12	8	6	3.887	1.720	44.3
13	8	5	3.752	1.696	45.2

Table 4.1: Homogeneity of all grid points for different Tx coil turn combinations. Hypotenuse: 25mm.

Number of turns			Average Inductance	Standard deviation	ratio
Tx1 high	Tx2 mid	Tx3 low	μ_M (μH)	σ (μH)	σ/μ_M %
9	8	7	5.823	0.985	16.9
10	8	6	5.720	0.806	14.1
11	8	5	5.564	0.790	14.2
11	8	6	5.784	0.778	13.4
12	8	5	5.614	0.792	14.1
12	8	6	5.834	0.762	13.1
13	8	5	5.654	0.799	14.1

Table 4.2: Homogeneity of 49 most inner points for different Tx coil turn combinations. Hypotenuse: 25mm.

Looking at Table 4.2 it seems that the turn combination that gives the most homogeneous inner area (measured by the ratio) is 12,8,6, decreasing the ratio by 2.8% in absolute terms compared to the initial turn combination.
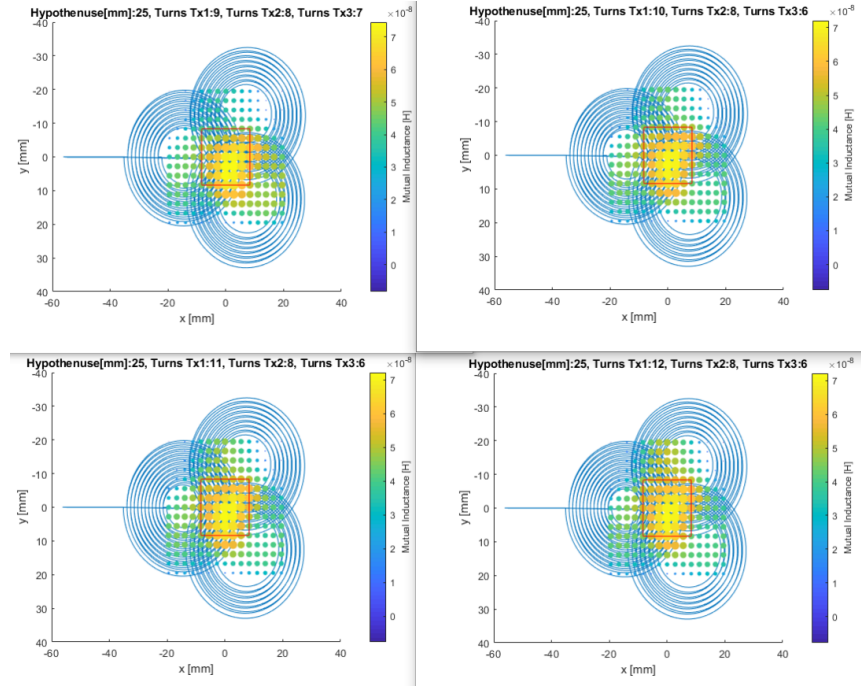
Figure 4.3: Map of mutual inductance for different turn combinations. Hypotenuse: 25mm

Comparing the images in Figure 4.3, it is quite difficult to detect any significant difference in the mutual inductance graphically for the various turn combinations.

Hypotenuse: 27.5mm

In this part, the hypotenuse of the equilateral triangle, drawn between the centers of the coils, was increased from 25 to 27.5mm. With the corresponding results presented in Tables 4.3 and 4.4, for all points and just the inner points, respectively. In Figure 4.4, the results are visualized as a heatmap.

Number of turns			Average Inductance	Standard deviation	Ratio
Tx1 high	Tx2 mid	Tx3 low	μ_M (μH)	σ (μH)	σ/μ_M %
9	8	7	3.555	1.518	42.7
10	8	6	3.472	1.380	39.8
11	8	6	3.521	1.400	39.8
12	8	6	3.887	1.720	44.3

Table 4.3: Homogeneity of all grid points for different Tx coil turn combinations. Hypotenuse: 27.5mm

| Number of turns | | | Average Inductance | Standard deviation | Ratio |
Tx1 high	Tx2 mid	Tx3 low	μ_M (μH)	σ (μH)	σ/μ_M %
9	8	7	4.577	0.775	16.9
10	8	6	4.509	0.507	11.2
11	8	6	4.553	0.462	10.1
12	8	6	4.587	0.432	9.4

Table 4.4: Homogeneity of 49 most inner points for different Tx coil turn combinations. Hypotenuse: 27.5mm
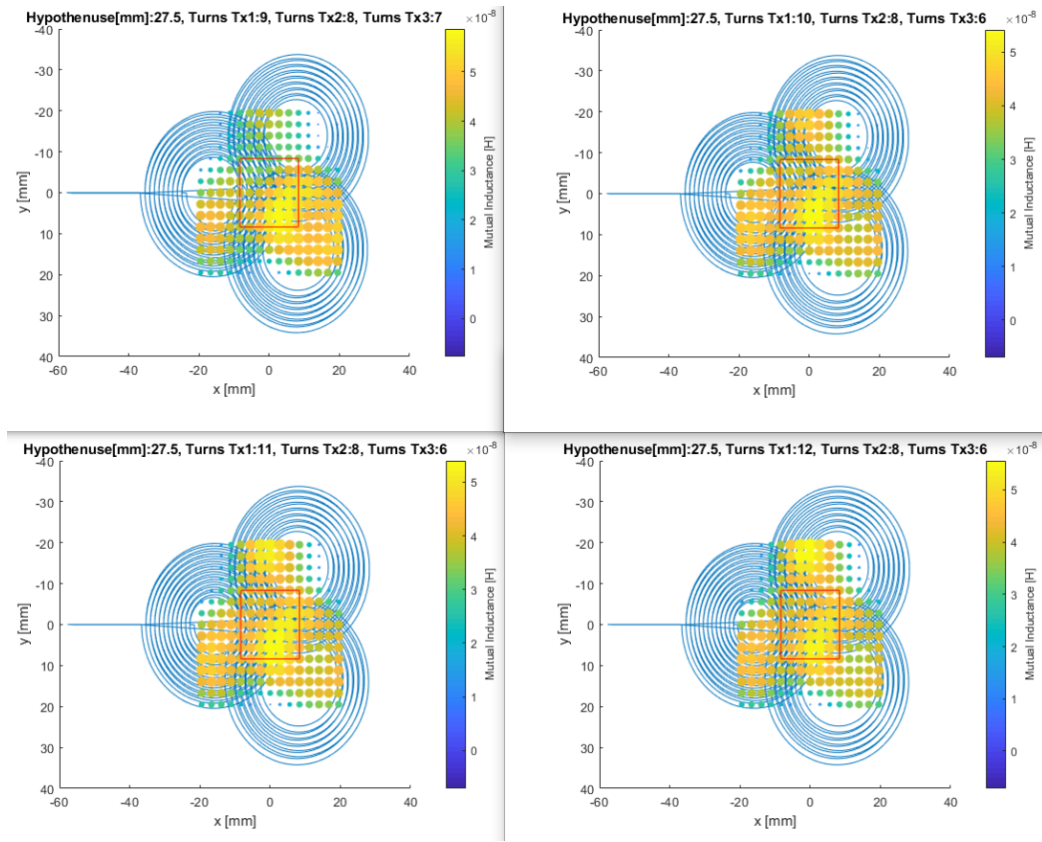
Figure 4.4: Map of mutual inductance for different Tx coil turn combinations. Hypotenuse = 27.5mm

Looking at Figure 4.4 and Table 4.4 and comparing them with Figure 4.3 and Table 4.2, it is observed that just moving the coils 2.5mm further apart for the initial setup did not improve the homogeneity. However for new turn combinations, at the new separation distance, the homogeneity is improved significantly. The best results for different separation distances (hypotenuses) from Table 4.2 and Table 4.4 were 13.1% and 9.4% respectively. This is an improvement of roughly 28% or 3.7% in absolute terms.

However the improvement in homogeneity was achieved at the cost of the average strength, with the mutual inductance (proportional to field strength) dropped from 5.834 to 4.587 μH, i.e roughly 21%. Hence to get the same induced voltage, the transmitter coil would require a larger coil current. One should keep in mind that these results are for the magnetostatic case that does not take into account physical wires, but only filamentary current traces.

Hypotenuse = 30mm

The separation distance between the coils, as measured by the hypotenuse of the equilateral triangle formed between the centers of the coils, was increased to 30mm. It is obvious from Figure 4.5 that this separation distance was too large. Hence the separation of the coil centers, with everything else being equal (distance to receiver 2mm (T2B) etc.), which gives the best result in the range of 30% to 60% larger than the outer radii of the coils (which is 19mm in this case).
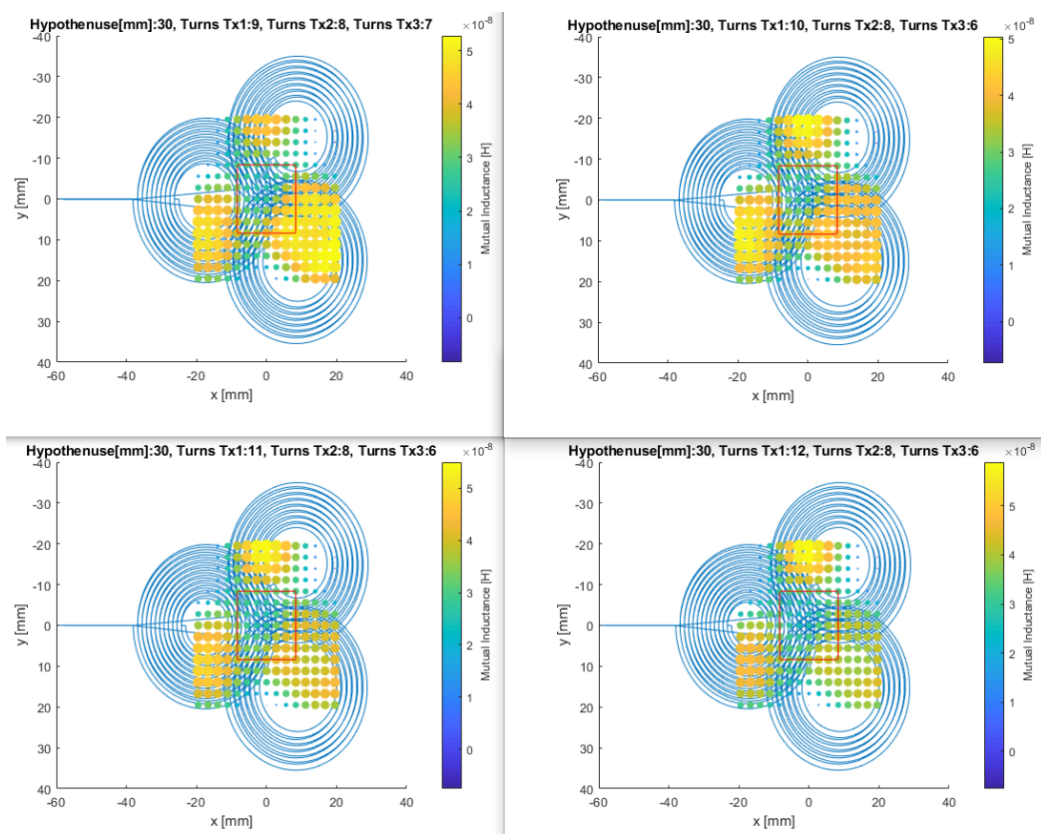
Figure 4.5: Map of mutual inductance. Hypotenuse = 30mm

4.2   Setup 2: Shared Area

From visualization of the electromagnetic simulations of setup 2 in Ansys Maxwell
(see Figure 4.6), it seems that a basic spiral coil creates a roughly homoge-
neous/uniform field at small z distances, in the region where it is enclosed by
two ferrite plates. In other words, the ferrite seem to compensate for the increased
distance from the conducting wires to the center which would otherwise weaken
the magnetic field. Therefore the ferrite plates seem to provide a low reluctance
path for the magnetic flux.
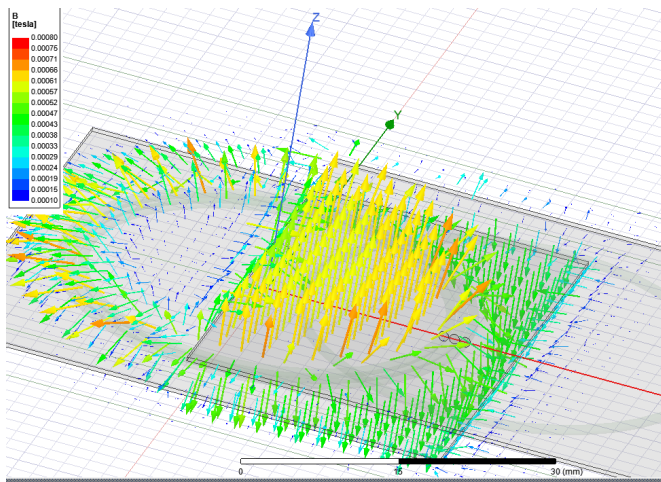
Figure 4.6: Misaligned coils with ferrite plates, z=1mm (T2B),
x=24mm
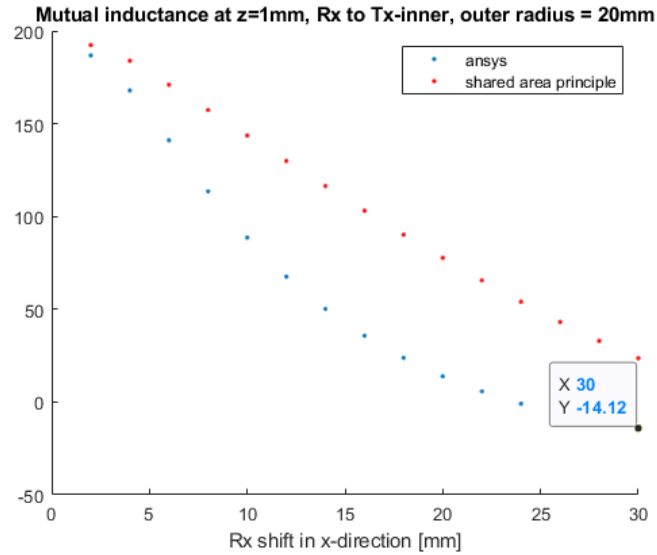
Figure 4.7: Misaligned coils with ferrite plates, z=1mm (T2B)

Looking at Figure 4.7, a negative mutual inductance value (in nH) can be observed as the receiver coil moves further away (more misalignment). This means that the dominating field lines are now entering from above instead of from below in the receiver coil, but also (assuming continuity) that there is some regions where the field lines are cancelling each other out perfectly.

We also note from Figure 4.7 that the mutual inductance quickly deviates from the "shared area principle" as misalignment increases. Ignoring the effect of the ferrite plate on the receiving end, if the magnetic field would have been homogeneous and only resided within the inner area of the loop, then the two curves should match completely.

4.3 Setup 3: Finite Ferrite
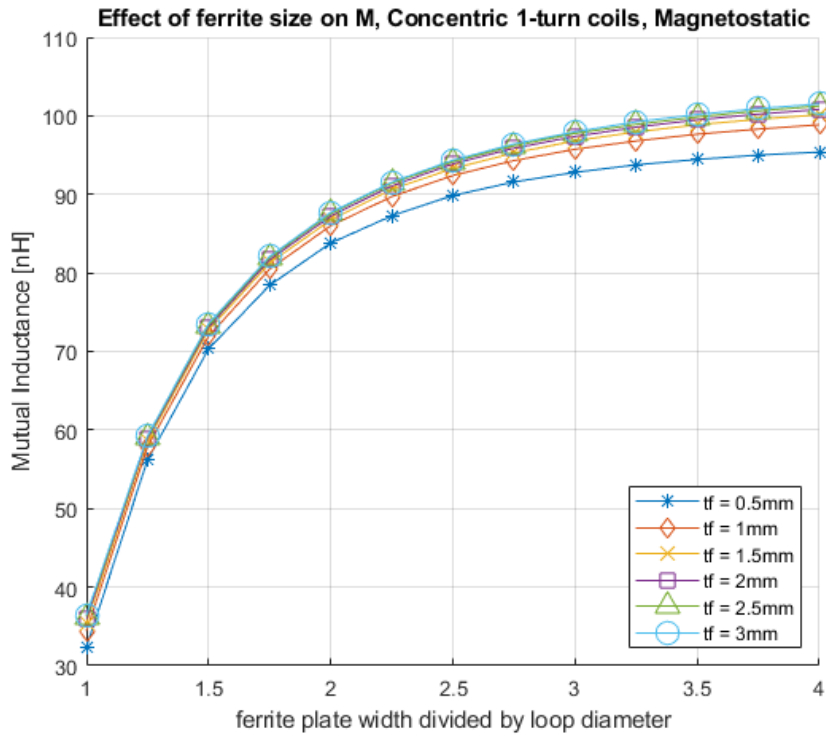
Figure 4.8: Effect of ferrite size

Figure 4.8 indicates that the ferrite plate width needs to be at least a factor of 2.5 larger than the outer diameter of the coil, for the infinite approximation to make sense, and preferably 3.5. This result differs from the 1.5 suggested by Roshen [10]. However, Roshen's results is for a larger coil of several turns, whereas these simulations were done using a very simple one-loop coil. Using additional loops may help to focus the magnetic field and hence produce different results.

M[nH]		Width factor			
		2.5	3	3.5	4
thickness factor	0.5	89.85	92.80	94.45	95.38
	1	92.41	95.75	97.66	98.86
	3	94.35	97.96	100.17	101.52

Table 4.5: Effect of ferrite size

The next step was to study the effect of ferrite plate thickness. The ferrite plate thicknesses were chosen in relation to the wire diameter of 1mm. Comparing the results in Table 4.5 for width factors 2.5 and 4 and a thickness factor of 1, 2.5 gives a roughly 7% lower value. Meanwhile, going from a width factor of 3.5 to 4 gives a difference of roughly 1%. The ferrite thickness seems to only have a minor influence, especially when it is at least as thick as the wire diameter.

4.4   Setup 4: Hurley-Duffy

In this part, the results the Matlab implementation of the algorithm in [9] is compared to the results from the original paper and simulations in Ansys Maxwell. In Table 4.6, the results from the original paper (closed form expression and FEM simulations) are presented under "Hurley-Duffy". The thesis' implementation results are presented under "Matlab", and the simulation results made in Ansys Maxwell for this paper are presented under "Ansys". Filament and Rectangular refer to two different implementations of attempted capture the behaviour of the rectangular cross-sectioned wires.

M [nH]	Matlab		Hurley-Duffy		
Frequency	Filament	Rectangular	Closed-form	FEM	Ansys
100kHz	10886	10780	10606	10680	10011
100MHz	10719	10611	10436	10450	6875

Table 4.6: Validation of implementation

Looking at Table 4.6, the large discrepancy between what the FEM simulation in the paper gave and what Ansys Maxwell gave for the high frequency could depend on that Hurley-Duffy, either deliberately did not include certain frequency dependant effects, or the Ansys Maxwell software has been updated with those features afterwards (the original FEM software were also from Ansys), since the paper is roughly 20 years old. The unknown size of the ferrites is also a possible explanation for the resulting lower values achieved from the simulations. The calculated results from the implementation in Matlab and the ones that the authors obtained are corresponding fairly well, with a difference of roughly 3%. However, the Matlab implementations seem to be slightly biased, overestimating the inductance compared to the original implementation.

4.5   Setup 5: Physical 12-turn Spiral

Calculating the mutual inductance with Matlab, using the expression of Hurley-Duffy [9], gave a value of $M = 25.8\mu H$. The results from electromagnetic simulations of the mutual inductance in Ansys Maxwell for varying ferrite widths are plotted in Figure 4.9
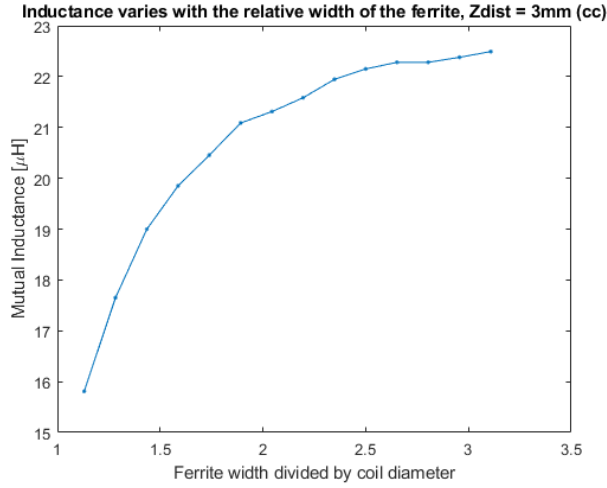
Figure 4.9: Inductance simulated in Ansys Maxwell for different ferrite widths, z=3mm (cc)

Looking at Figure 4.9, it seems that inductance is converging towards roughly 22.5-23μH. This can be compared to the result from simulation in Matlab of 25.8μH, which assumes infinite ferrite plates. Ideally the data should converge to the same value. Hence, there seems to be a small bias in the Matlab expression. For example, the Hurley-Duffy expression (assuming infinite ferrites) gave, an error of roughly 15%, compared to the simulation made in Ansys Maxwell, for a ferrite width factor of 3.

4.5.1   Misalignment

Tables 4.7 and 4.8 show the measured values and the simulated values in Ansys Maxwell, respectively, for misalignments of the coils in setup 5 with an inner and outer radii of roughly 10mm and 23mm, respectively.

x displacement	0mm	2mm	4mm	6mm	8mm	10mm	12mm	14mm
M [μH]		16.93	16.63	16.26	15.20	13.40	11.49	9.53	7.53

Table 4.7: Measured values on physical coil

x displacement	0mm	2mm	4mm	6mm	8mm	10mm	12mm	14mm
M [μH]		15.81	15.53	14.68	13.37	11.69	9.83	7.83	5.84

Table 4.8: Simulated values in Ansys Maxwell

In Figure 4.10 the measured and simulated (in Ansys Maxwell) values for the misalignment are plotted (the two lower lines). The other lines used the result from the Hurley-Duffy expression for the concentric case as a starting point, but then used the shared area to scale the values for three different areas defined by different radii (upper three lines).
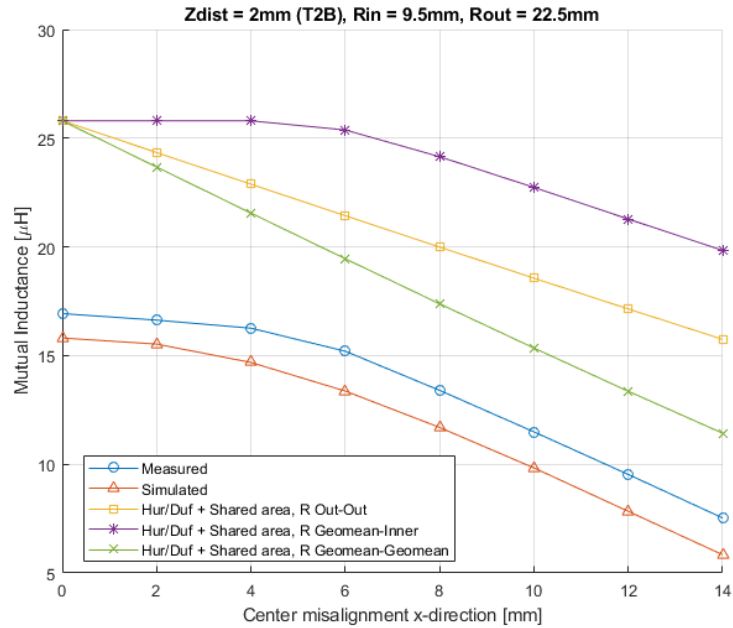

Figure 4.10: Mutual inductance for misaligned coils, z=2mm (T2B)

The clear bias between the simulated values from Ansys Maxwell (lowest, red) and the measured (second lowest, blue) plotted in Figure 4.10, is most probably caused by the small ferrite core which was not included in the Ansys Maxwell simulation. The Hurley-Duffy implementation in Matlab is significantly overestimating the mutual inductance (M) since it assumes infinite ferrite plates.

It can be seen in Figure 4.10 that the mutual inductance does not change very much for minor misalignments. This can be related to the inner and outer diameters of the spiral coils. The turns are covering slightly more than half of the area inside the outer one. Roughly 13mm of the total radius of 23mm is covered by wires.

In the area covered by wires, the wires will actually have a field cancelling effect on each other, since the inner wire will generate a field pointing in the opposite direction on the outer neighbouring wires, as compared to the field entering the wire-free region of the coil. Hence, the full additive effect of the fields from all the wires contributing to the total magnetic field occur mainly in the inner area that is free from wires. This is something that would not occur the same way in a solenoidal coil.

Looking at the lines for the shared area principle, it seems that calculating the shared area for a circle of the geometric mean radius (approximately 14.6mm), gives the correct slope after passing the 6mm misalignment, corresponding to 26% of the outer radius. On the other hand, calculating the shared area between the loops using the geometric mean radius and the inner radius, seems to capture better the mutual inductance behavior when the misalignment starts to increase.

In Figure 4.11, the measured and simulated values from Ansys Maxwell are compared to the shared area principle again. But here the Ansys simulated value for the concentric case is used as start point. The dashed line "R:combo", is a linearly weighted version of "R:geo-in" and "R:geo:geo", where the weights are the normalized misaligned x-positions, as such: [0:2:14]/14. It weights "R:geo-in" heavier in the beginning and it then shifts more weight to "R:geo-geo" as misalignment increases.
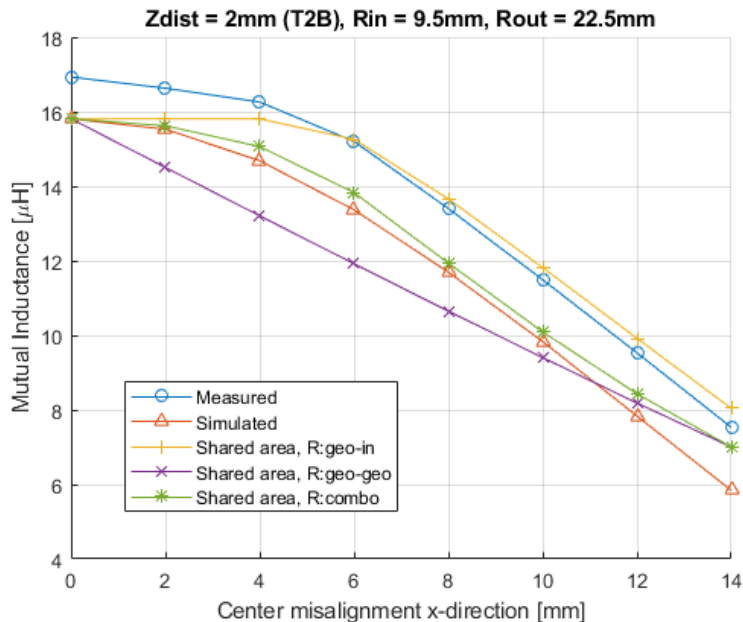
Figure 4.11: Mutual inductance for misaligned receiver, z=2mm (T2B)

Both "R:geo-in" and "R:combo" are consistently overestimating the mutual inductance comparing to the values from the Ansys Maxwell simulations. However the average error percentage for "R:combo" is 4.9%, while for "R:geo-in" it's 15.6%. With a standard deviation of 6.5% and 12.7% respectively. It also worth noting that "R:combo" starts to deviate from the simulated Ansys Maxwell data for misalignments beyond 10 mm.

Summary

This thesis work focused on two different areas: The impact of ferrite plates on the mutual inductance of two coils and the possibility of creating a homogenized magnetic field for more uniform spatial coupling.

5.1 Homogenized B-field

It was found that the homogeneity of the initial coil setup can be improved for a small area around the coil system center (for a tri-coil configuration). The achieved improvement was 28%, but it also gave a 21% drop in the maximum strength of the field within the area. It was also found that the optimal separation distance between the coil-centers, from a homogeneous field perspective, was between 30% to 60% larger than the outer coil radius.

5.2 Effect of Ferrite Plates

5.2.1 Misalignment and shared area

For small separation distances in z, it seems that a weighted combination of shared area calculations can capture the behaviour/change of the mutual inductance very well, in the case of lateral coil misalignment. The average percentage error is only 4.9%, assuming the initial concentric coil value (i.e., mutual inductance for no misalignment) is known. However these results of using the geometric mean are probably very specific to the identical planar spiral coils used in this thesis. Looking at the basic case of one turn or a few turns in setup 2, the shared area principle has not been found to give a good fit to the full-wave simulation results for lateral misalignments.

5.2.2   Size of ferrite

It was found that the ferrite thickness had a marginal impact on the mutual inductance, when the thickness was half the wire diameter. Specifically, the mutual inductance changed by 7% as the ferrite width increased from 2.5 to 4 times of the coil diameter. The mutual inductance seems to converge for a ferrite width of a factor 4 of the outer coil diameter and hence was deemed a good size for the infinite ferrite plate assumption. In contrast, Roshen has previously found that a factor 1.5 would be sufficient to fulfill this assumption [10]. This may be due to this thesis using one-loop coils in the study, whereas Roshen used several turns, which probably helped to focus the magnetic field on a smaller area.

5.3   Future Work

Trying to equalize the magnetic field just by adding the number of inner turns had varying impact for small changes in the hypotenuse of the equilateral triangle that defined the placement of the three transmitter coils. For future work, one could automate the process of optimizing the homogeneity of the field through the use of more variables (e.g., adding turns on the outside as well, placement of coils, how tightly wound the wire is, varying the height where field is measured, etc.). One can add more coils in more complicated systems. On the question of measuring the homogeneity, there may exist better performance measures than the ratio of standard deviation to the mean. One could also choose to homogenize the points forming a triangle between the coil centers instead. This could enable the placement of these modules of 3-coil systems next to each other to cover a larger area, like a honeycomb.

A further step would be to test if the results for the field homogeneity work would still hold for case with ferrite plates. Hypothetically, as long as the ferrite only enhances and do not "bend" the flux lines too much, the results should hold.

For the shared area principle, a very specific formula was found for identical planar spiral coils. For future work it would be good to see how general the results are, and if there is a similar way of handling solenoidal coils.

References

[1] Matlab: `https://se.mathworks.com/products/matlab.html`
[Accessed 2019-05-29]

[2] Ansys-Maxwell, an electromagnetic simulation software:
`https://www.ansys.com/products/electronics/ansys-maxwell`
[Accessed: 2019-05-29]

[3] D.K. Kithany, "Wireless Power Market Tracker", 2019-04-22. [Online]. Available:
`https://technology.ihs.com/584705/wireless-power-market-tracker`
[Accessed 2019-05-31]

[4] Wikiversity. [Online].
Available: `https://en.wikiversity.org/wiki/Fundamental_Physics/Electricity/Transformer`
[Accessed: 2019-05-31]

[5] Wireless Power Consortium: "Magnetic Resonance and Magnetic Induction - making the right choice for your application". [Online]. Available:
`https://www.wirelesspowerconsortium.com/knowledge-base/`
`magnetic-induction-technology/resonance/`
`magnetic-resonance-and-magnetic-induction-`
`making-the-right-choice-for-your-application.html`
[Accessed 2019-05-31]

[6] Mutual Inductance Calculation Between Circular Filaments Arbitrarily Positioned in Space: Alternative to Grover's Formula
Slobodan Babic, Frédéric Sirois, Cevdet Akyel, and Claudio Girardi
Published in: IEEE Transactions on Magnetics, Volume: 46, Issue: 9, September 2010

[7] Simple Analytic Expressions for the Magnetic Field of a Circular Current Loop
James Simpson. John Lane, Chrstopher Immer and Robert Youngquist
Published: 2001-01-01
`https://ntrs.nasa.gov/search.jsp?R=20010038494`
[Accessed: 2019-05-24]

[8]   Analysis of Inductive Coupling Wireless Power Transfer Systems
      Arianna Ginette Amaya Colina
      Published: Master's Thesis Lund University, Department of Electrical and
      Information Technology, 2018

[9]   Calculation of Self- and Mutual Impedances in Planar Sandwich Inductors
      William Gerard Hurley, and Maeve C. Duffy
      Published in: IEEE Transactions on Magnetics, Volume: 33, Issue: 3, May
      1997

[10] Analysis of Planar Sandwich Inductors by Current Images
      Waseem A. Roshen
      Published in: IEEE Transactions on Magnetics, Volume: 26, Issue: 5,
      September 1990

[11] D.K. Cheng, Field and Wave Electromagnetics, Second Edition, Addison-
      Wesley, 1989.

[12] Modelling of Inductive effects in Thin Wire Coils
      F. Delince, P. Dular, A. Genon, W. Legros, J. Mauhin, A. Nicolet
      Published in: IEEE Transactions on Magnetics, Volume: 28, Issue: 2, March
      1992

[13] Optimization Procedure of Complex Permeability for a Wireless Power Trans-
      fer System
      Hongseok Kim, Chiuk Song, Jiseong Kim, Hak Byoung Park, Hyun Ho Park,
      Eakhwan Song and Joungho Kmi
      Published: 2013 Asia-Pacific Symposium on Electromagnetic Compatibility
      (APEMC)

[14] Mutual Inductance and Inductance Calculations by Maxwell's Method
      Antonio Carlos M. de Queiroz
      `http://www.coe.ufrj.br/~acmq/tesla/maxwell.pdf` [Accessed 2019-05-
      29]

[15] Calculation of Self- and Mutual Impedances in Planar Magnetic Structures
      William Gerard Hurley, and Maeve C. Duffy
      Published in: IEEE Transactions on Magnetics, Volume: 31, Issue: 4, July
      1995

[16] Physical measurement of mutual induction:
      `http://denverpels.org/Downloads/Denver_PELS_20070410_Hesterman_`
      `Magnetic_Coupling.pdf` [Accessed 2019-05-29]

[17] TEM Wave Properties of Microstrip Transmission Lines
      P. Silvester
      Published in: Proceedings of IEE, Vol: 115, January 1968

[18] Effect of Finite Thickness of Magnetic Substrate on Planar Inductors
      Waseem A. Roshen
      Published in: IEEE Transactions on Magnetics, Volume: 26, Issue: 1, January
      1990

[19] Wolfram. [Online].
     Available: `http://mathworld.wolfram.com/CylindricalCoordinates.`
     `html` [Accessed: 2019-06-01]

Hurley-Duffy

This part gives the full expression of the mutual impedance due to the presence of the ferrites as derived in [9], i.e.,

$$Z_{sw}^p = \frac{j\omega\mu_0\pi}{h_1 ln(r_2/r_1)h_2 ln(a_2/a_1)} \ldots$$

$$\int_{k=0}^{\infty} S(kr_2, kr_1)S(ka_2, ka_1)[f(\lambda) + g(\lambda)]Q(kh_1, kh_2)dk.$$

(A.1)

This expression assumes a current distribution in the cross-section to be only depending on the radius: $J(r) = \frac{I}{hr \cdot ln(r_2/r_1)}$ and assuming that the wires are solid, perfect conductors.

$\lambda(t_f)$ is a function of the ferrite thicknesses and $f(\lambda)$,$g(\lambda)$ also relates to the influence of the ferrite plates given their distances to the respective coils. Q and S both relate to the geometry of the wires.

r_1, r_2 inner,outer radius of primary coil

a_1, a_2 inner,outer radius of secondary coil

h_1, h_2 height of primary relative to the secondary coil wire

$\phi(k) = \frac{\mu_r - \eta/k}{\mu_r + \eta/k}$, $\eta(k) = \sqrt{k^2 + j\omega\mu_0\mu_r\sigma}$

$\lambda(t_f) = \phi(k)\frac{1 - e^{2\eta t_f}}{1 - \phi^2(k)e^{2\eta t_f}}$, $S(kx, ky) = \frac{J_0(kx) - J_0(ky)}{k}$

$J_\nu(\cdot) =$ bessel function of first kind, degree ν.

$Q(kx, ky) = \frac{2}{k^2}[cosh(0.5k(x+y)) - cosh(0.5k(x-y))]$

$$f(\lambda) = \frac{\lambda(t_1)e^{-k(d_1+d_2)} + \lambda(t_2)e^{-k(d_1'+d_2')}}{1 - \lambda(t_1)\lambda(t_2)e^{-2ks}}$$

$$g(\lambda) = \frac{\lambda(t_1)e^{-2ks} \cdot cosh(k(d_2 - d_1))}{1 - \lambda(t_1)\lambda(t_2)e^{-2ks}}$$

$d_1' = s - d_1, d_2' = s - d_2$, $s =$ distance between ferrite plates, $d_1 =$ distance between first ferrite plate and primary coil, $d_2 =$ distance between first ferrite plate and secondary coil.

LUND
UNIVERSITY